Surface Chemistry

DOI: 10.1002/ange.200600075

Facile Monolayer Assembly of Fluorophore-Containing Zeolite Rods in Uniform Orientations for Anisotropic Photoluminescence**

Jin Seok Lee, Hyunjin Lim, Kwang Ha,
*Hyeonsik Cheong, and Kyung Byung Yoon**

Microparticles, like atoms, small molecules, and nanoparticles, will someday be used routinely in chemistry and materials science as a class of building blocks. It is therefore necessary to start developing methods for organizing them into larger organized entities and to explore practical applications of the organized entities.[1–4] Thus, zeolite microcrystals have been organized in the form of monolayers on various substrates. For example, Mallouk and co-workers covalently assembled monolayers of zeolite Y mircrocrystals on the surface of SnO_2-coated glass electrodes by using dimethoxysilyl groups as tethers.[5] Yan and Bein similarly assembled monolayers of zeolite A crystals on gold electrodes through trimethoxysilyl tethers.[6] Calzaferri and co-workers assembled monolayers of zeolite A microcrystals on glassy carbon electrodes by using polystyrene as the glue.[7] Tsapatsis and co-workers assembled monolayers of zeolite A crystals on Si substrates through ionic linkages between the substrates and zeolite microcrystals.[8] The research groups of Calzaferri,[9] Tsapatsis,[8] as well as Ban and Takahashi[10] also demonstrated the assembly of a monolayer of zeolite A microcrystals through physical adsorption of the zeolite crystals onto substrates through slow evaporation of droplets of aqueous solutions of zeolite microparticles placed on substrates or by dip-coating the substrates. Similarly, Bein and co-workers demonstrated the aligned growth of zincophosphate crystals on substrates.[11]

We have developed methods for organizing zeolite microcrystals in the form of uniformly aligned monolayers on various substrates by inducing well-defined molecular linkages between each microcrystal and the substrates.[12–19] The resulting monolayers show high degrees of coverage, high degrees of close packing between the attached crystals, strong binding between the crystals and substrates, and high degrees of uniform orientation of the crystals. The zeolite monolayers have served as supramolecularly organized light-harvesting systems[20,21] and as excellent precursors for the preparation of continuous zeolite films with uniform orientations of the nanopores or nanochannels. The latter property makes the monolayers suitable for application as molecular sieving membranes[22,23] and nonlinear optical films.[24] The assembly of monolayers of zeolite microcrystals has also been regarded as one of the future directions of zeolite research.[25]

In our approaches, the monolayers have mostly been assembled by refluxing solutions of bare or functional-group-tethered zeolite crystals in toluene in the presence of substrates bearing functional groups.[12–18] The solutions were often stirred to keep them dispersed and to give them kinetic energy. More than 24 h were usually required to cover the majority (> 90 %) of the 4 cm^2 glass plates with closely packed monolayers. High degrees (> 98 %) of uniform orientation were obtained when the aspect ratios of the zeolite microcrystals were equal to or less than 1. However, the reflux/stirring (RS) method did not produce high coverage and uniform orientation in the case of cylindrical zeolite microcrystals with aspect ratios higher than 1. We recently discovered that sonication of the stacks of bare glass/3-chloropropyl-coated glass (CP-g)/bare glass plates in a toluene solution dispersed with bare zeolite crystals leads to the 4 cm^2 glass plates being fully covered with very tightly packed monolayers of zeolite microcrystals within two minutes.[19] This method was named "sonication with stacking" (SS). We now report that the SS method is also highly effective for assembling cylindrical zeolite crystals with aspect ratios of up to 3 in vertically oriented monolayers, and that the monolayers give anisotropic photoluminescence in a high dichroic ratio, when fluorescent molecules were incorporated in the channels of zeolite L along the channel directions. The crystals self-assembled into horizontally oriented monolayers when the zeolite L crystals had a hexagonal columnar morphology.

Cylindrical zeolite L crystals with dimensions of 1 × 2–3 μm (diameter × length) and hexagonal columnar zeolite L crystals of 1 × 4–5 μm (width × length) used in the current study were prepared according to procedures described previously.[26] Pyronin B ions (PyB^+, Figure 1 a) were incorporated into the channels of zeolite L crystals by ion exchange of the K^+ ions of the zeolites with PyB^+ ions in water. Since the length of the PyB^+ ion (16.3 Å) is longer than the width of the zeolite L lobe (12.6 Å, Figure 1 b), the incorporated PyB^+ ions are likely to be lined up along the direction of the channel (Figure 1 c) with a tilt angle of less than 20°.[21] The surfaces of the PyB^+-containing zeolite L [$(PyB^+)L$] crystals were subsequently treated with (3-aminopropyl)trimethoxysilane (AP-TMS) to tether 3-aminopropyl (AP) groups onto their surfaces and to prevent the egress of the incorporated PyB^+

---

[*] J. S. Lee, Dr. K. Ha, Prof. Dr. K. B. Yoon
Center for Microcrystal Assembly
Department of Chemistry
and Program of Integrated Biotechnology
Sogang University
Seoul 121-742 (Korea)
Fax: (+82) 2-706-4269
E-mail: yoonkb@sogang.ac.kr
H. Lim, Prof. Dr. H. Cheong
Department of Physics
Sogang University
Seoul 121-742 (Korea)

[**] We thank the Ministry of Science and Technology (MOST) and Sogang University for supporting this work through the Creative Research Initiatives (CRI) and the Internal Research Fund programs, respectively. H.C. and H.L. also thank the Quantum Photonic Science Research Center supported by the Korea Science and Engineering Foundation.

Supporting information for this article is available on the WWW under http://www.angewandte.org or from the author.

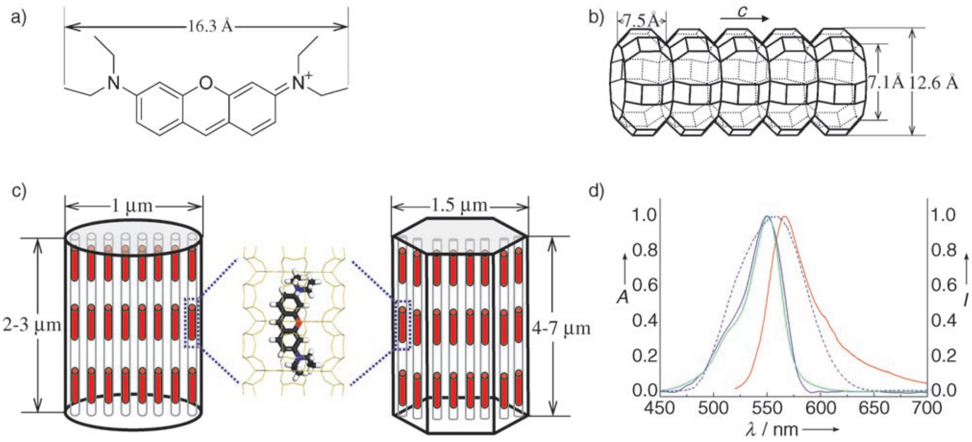

Figure 1. a) Molecular structure of the PyB^+ ion. The estimated length is 16.3 Å. b) The zeolite L channel consists of 7.5 Å long lobes with a pore opening of 7.1 Å. The internal width of a lobe is 12.6 Å, which is smaller than the length of the PyB^+ ion. c) Illustrations of PyB^+-containing cylindrical (left) and hexagonal columnar (right) zeolite L crystals with their dimensions. The red cylinders represent PyB^+ ions positioned in the channel direction. The middle diagram illustrates the imagined position of a PyB^+ ion positioned in the channel direction. d) The diffuse-reflectance spectrum of PyB^+-containing zeolite L crystals (blue dashed curve, $\lambda_{max} = 558$ nm), the excitation spectrum of PyB^+-containing zeolite L crystals dispersed in glycerol (solid blue curve, $\lambda_{max} = 550$ nm), the absorption spectrum of PyB^+ in methanol (green curve, $\lambda_{max} = 551$ nm), and the isotropic fluorescence spectrum of PyB^+-containing zeolite L crystals dispersed in glycerol (red curve, $\lambda_{E_{max}} = 567$ nm).

ions from the channels into the solution (glycerol) during the measurement of the anisotropic photoluminescence. CP-g plates (1.8×1.8 cm^2) were prepared by treating bare glass plates with (3-chloropropyl)trimethoxysilane (CP-TMS). The diffuse-reflectance absorption spectrum of the dry $(PyB^+)L$ crystals and the fluorescence spectra of $(PyB^+)L$ crystals dispersed in glycerol are shown in Figure 1 d.

When cylindrical AP-coated $(PyB^+)L$ (cyl-AP-$(PyB^+)L$) crystals were attached onto CP-g plates by the SS method over two minutes the crystals self-assembled very tightly and vertically, as shown by scanning electron microscopy (SEM; Figure 2 a). In contrast, hexagonal columnar AP-coated $(PyB^+)L$ (hex-AP-$(PyB^+)L$) crystals self-assembled horizontally (Figure 2 b). Such a difference in orientation arises from the tendency of the microcrystals to be attached onto substrates through their largest face (Figure 3). Consistent with the SEM images, X-ray diffraction of the monolayers of cyl-AP-$(PyB^+)L$ crystals show signals only from the (00*c*) planes (Figure 2 c), while the monolayers of hex-AP-$(PyB^+)L$ crystals give signals only from the (*a*00) planes (Figure 2 d). The X-ray data revealed that the degrees of uniform orientation on the 4-cm^2 glass plates were higher than 99.9 %.

The degree of close packing and the degree of vertical orientation of cyl-AP-$(PyB^+)L$ crystals decreased significantly when the monolayer assembly was carried out for two minutes by sonication but without interposing the CP-g plates between the bare glass plates (SW method; Figure 2 e). When the RS method was applied instead of the SS and SW methods, the degree of close packing was very poor and the crystals tended to attach onto the CP-g plates horizontally (Figure 2 f), even after reaction for 24 h. The above two results reveal that strong agitation is very important to attach long cylindrical microcrystals vertically and for the remarkable superiority of the SS method over SW and RS methods in terms of coverage, close packing, and uniform orientation during the assembly of a monolayer of long cylindrical microcrystals in the upright position.

The CP-g plate covered with cyl-AP-$(PyB^+)L$ crystals on both sides in vertical orientations is denoted as v-$(PyB^+)L$-g. The normalized polarized fluorescence spectra obtained from v-$(PyB^+)L$-g are shown in Figure 4 a. The vertical and horizontal components of the fluorescence spectrum obtained by exciting the v-$(PyB^+)L$-g stacks with vertically and horizontally polarized laser beams (514.5 nm) are denoted as S_{vVV}, S_{vVH}, S_{vHV}, and S_{vHH}. The subscripts represent the orientation of the zeolite L crystal on the glass, the orientation of the polarized incident light, and the orientation of the polarizer to the detector, respectively.

The corresponding intensities at the maximum-emission wavelengths ($\lambda_{E_{max}}$) are denoted as I_{vVV}, I_{vVH}, I_{vHV}, and I_{vHH}, respectively, with $\lambda_{E_{max}}$ values of 567, 570, 570, and 570 nm, respectively. The $\lambda_{E_{max}}$ value of PyB^+ in glycerol (S_{GL}) was 577 nm, and the corresponding band widths (W_{fwhm}) were 0.18, 0.23, 0.24, 0.23, and 0.16 eV, respectively. Since all the PyB^+ ions residing within the channels are vertically oriented, they are excited only by vertically polarized light and the fluorescence from them must also be vertically polarized. Therefore, the S_{vVH}, S_{vHV}, and S_{vHH} bands are assigned as those arising from randomly oriented PyB^+ ions on the external surfaces. The similarities of the $\lambda_{E_{max}}$ (570 nm) and W_{fwhm} values (ca. 0.23 eV) also support this assignment (see the Supporting Information). The blue shift of the S_{vVV} band relative to those of S_{vVH}, S_{vHV}, and S_{vHH} is attributed to the confinement effect of the ion in the narrow channel.[27]

Figure 4 b shows the anisotropic fluorescence spectra for S_{vVV} and S_{vVH}. The inset shows the angle-dependent change of $I_{vV\theta}/I_{vVH}$, where $I_{vV\theta}$ represents the intensity of the spectrum of v-$(PyB^+)L$-g at $\lambda_{E_{max}}$ at various angles (θ) under vertical excitation. The I_{vVV}/I_{vVH} ratio was 8.9:1, which is about double that obtained by Tolbert and co-workers (4.5:1) for polymer-containing mesoporous silica.[28,29] Thus, this current study demonstrates a novel and highly effective way of preparing supramolecularly organized systems that give strongly anisotropic photoluminescence. Figure 4 c shows the anisotropic fluorescence spectra of the S_{vHH} and S_{vHV} components. The inset shows the angle-dependent change of $I_{vH\theta}/I_{vHV}$, where $I_{vH\theta}$ represents the intensity of the spectrum of v-$(PyB^+)L$-g at $\lambda_{E_{max}}$ at various values of θ under horizontal excitation.

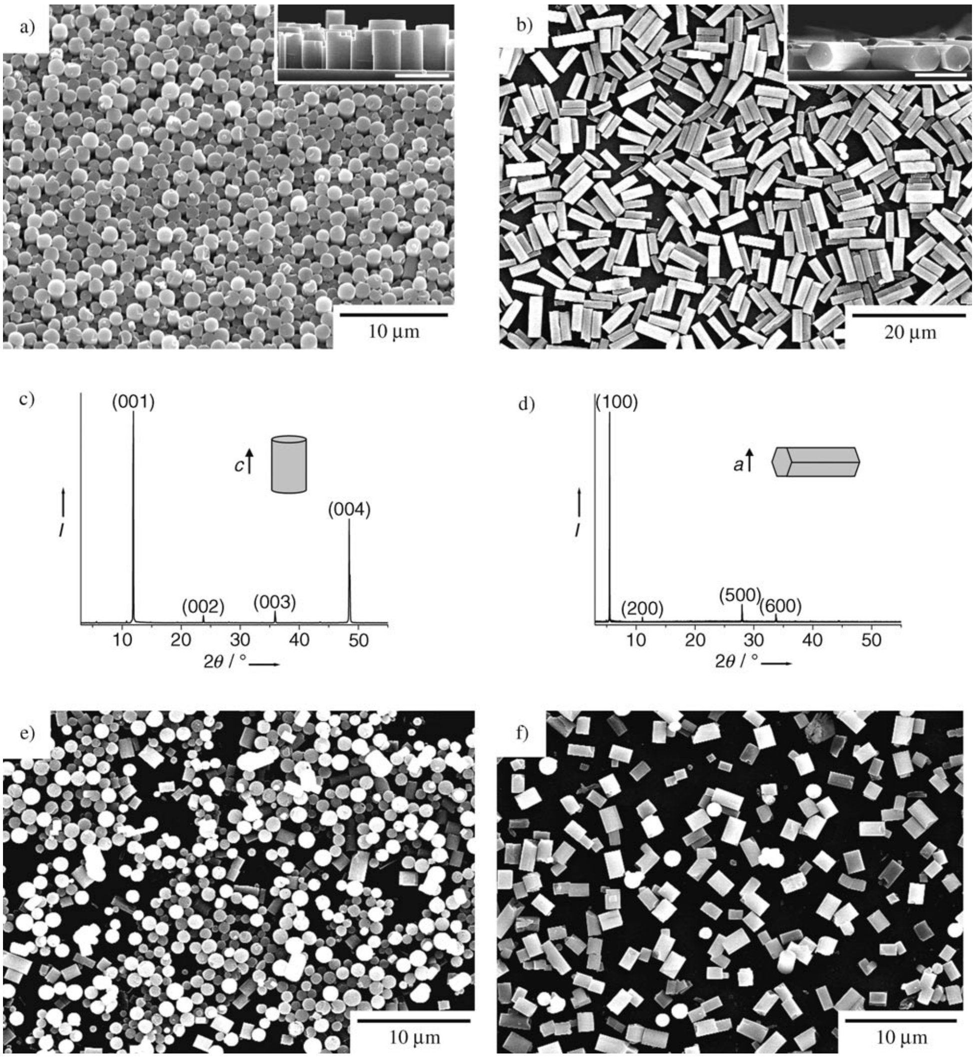

Figure 2. a) SEM image of v-(PyB$^+$)L-g showing the very tight close packing and vertical orientations of the zeolite L crsytals. The inset shows an SEM image of the cross-section. Scale bar = 2 μm. b) SEM image of h-(PyB$^+$)L-g. The inset shows an SEM image of the cross-section. Scale bar = 2 μm. c) X-ray diffraction pattern of v-(PyB$^+$)L-g showing the diffraction lines from (00*c*) planes of zeolite L with $c = 1$, 2, 3, and 4 at $2\theta = 11.9$, 23.8, 35.9, and 48.5°, respectively. d) X-ray diffraction pattern of h-(PyB$^+$)L-g showing the diffraction lines from (*a*00) planes of zeolite L with $a = 1$, 2, 5, and 6 at $2\theta = 5.5$, 11.1, 28.0, and 33.7°, respectively. The absence of diffraction lines arising from (300) and (400) planes occurs because their intrinsic intensities are very small, that is, 0.7 and 1.5% with respect to the diffraction intensity of the (100) plane. e) SEM image of the monolayer of cyl-AP-(PyB$^+$)L crystals assembled on CP-g by the SW method for 2 min showing that the poor degrees of close packing and vertical orientation. f) SEM image of the monolayer of cyl-AP-(PyB$^+$)L crystals assembled on CP-g by the RS method over 24 h.

The $I_{\mathrm{vHH}}/I_{\mathrm{vHV}}$ ratio was 1.8:1, which is smaller than that of the PyB$^+$ ion in glycerol (2.8:1, see the Supporting Information). This result may arise as a consequence of faster energy transfer between the external PyB$^+$ ions as a result of aggregation. Furthermore, the average $I_{\mathrm{vVH}}/I_{\mathrm{vHV}}$ ratio was 1.8:1. This value indicates that 44% of the value of I_{vVH} arises from energy transfer from intrachannel PyB$^+$ ions to the external PyB$^+$ ions. The fact that the W_{fwhm} value of the S_{vVH} band is greater than that of S_{vVV} at longer wavelength regions (Figure 4a) and that $\lambda_{E_{\max}}$ is shorter for S_{vVV} than S_{vVH} further support a directional energy transfer. As noted, the direction of energy transfer is opposite to the case reported by Tolbert and co-workers.[28]

The CP-g plate covered with hex-AP-(PyB$^+$)L crystals on both sides in horizontal orientations is denoted as h-(PyB$^+$)L-g. The four polarized fluorescence spectra obtained from a stack of three h-(PyB$^+$)L-g are denoted as S_{hHH}, S_{hHV}, S_{hVH}, and S_{hVV} (see the Supporting Information for spectra). The corresponding intensities at $\lambda_{E_{\max}}$ are denoted as I_{hHH}, I_{hHV}, I_{hVH}, and I_{hVV}. The $I_{\mathrm{hHH}}/I_{\mathrm{hHV}}$ ratio was 3.0:1. The reason for the $I_{\mathrm{hHH}}/I_{\mathrm{hHV}}$ ratio being about 1/3 of that of $I_{\mathrm{vVV}}/I_{\mathrm{vVH}}$ (8.9:1) is because the hex-AP-(PyB$^+$)L crystals are oriented randomly on the glass plane, even though they are all horizontally attached to the glass plane, and the integration of $(\cos\theta)^2$ over the angle range 0–180° gives 1/3. If the hex-AP-(PyB$^+$)L crystals were uniformly oriented in the x and y directions as well, then the $I_{\mathrm{hHH}}/I_{\mathrm{hHV}}$ ratio would be approximately 9:1.

Although the assembly of monolayers of zeolite rods in a vertical orientation has been recognized as being important because of the applicability of the aligned zeolite rods to second harmonic generation, molecular sieve membranes, and macroscopic alignments of guest molecules, only a few examples have been reported. Caro et al. developed a method driven by an electric field to vertically orient the related long MFI-type zeolite rods.[30] Chao and co-workers used anodized alumina discs to grow vertical metal-doped aluminophosphate molecular sieves.[31] However, the degrees of close packing and uniform orientation achieved by the above cases cannot compete with those of v-(PyB$^+$)L-g.

In conclusion, we have described how zeolite L monolayers can be prepared on glass in two orientations. The organized monolayers can be applied as novel supramolecularly organized systems for the demonstration of anisotropic photoluminescence in high dichroic ratios,[32] to study energy-transfer dynamics between internally and externally placed fluorophores,[33,34] and to develop zeolite-based advanced materials. The vertically assembled zeolite L monolayers also have the potential to be transformed into continuous films with one-dimensional channels all oriented perpendicular to the substrate, an arrangement that has been shown to be very difficult to obtain.[35]

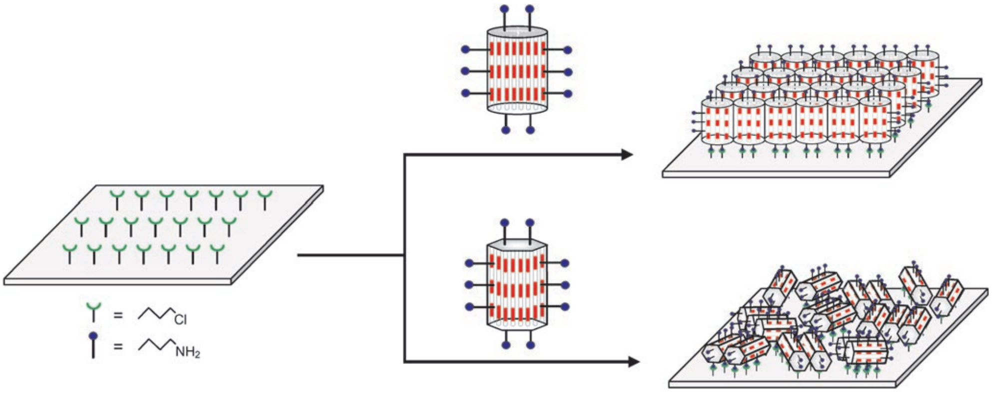

Figure 3. Schematic illustration of the morphology-dependent change of the orientation of zeolite L crystals during assembly of the monolayer by the SS method. While the cyl-AP-(PyB$^+$)L crystals assemble into a vertically oriented monolayer, the hex-AP-(PyB$^+$)L crystals assemble into a horizontally oriented monolayer on CP-g plates.

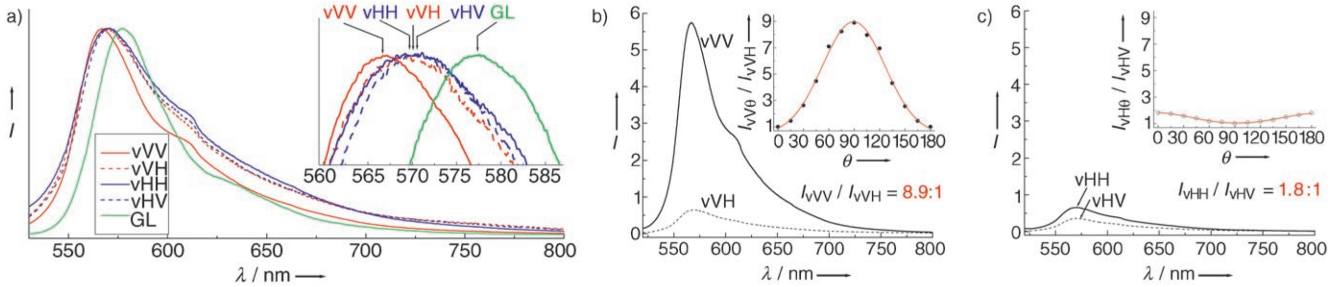

Figure 4. Anisotropic fluorescence spectra and dichroic ratios: a) Normalized anisotropic fluorescence spectra (S_{vVV}, S_{vVH}, S_{vHV}, and S_{vHH}) of v-(PyB$^+$)L-g and the fluorescence spectrum of the 1 μM solution of PyB$^+$ ions in glycerol (S_{GL}). The inset shows the peak positions of the spectra. b) S_{vVV} and S_{vVH}. c) S_{vHH} and S_{vHV}. The insets in (b) and (c) show the angle-dependent changes of $I_{vV\theta}/I_{vVH}$ and $I_{vH\theta}/I_{vHV}$, respectively.

Experimental Section

Materials: The cylindrical and hexagonal columnar zeolite L crystals were prepared according to procedures described previously.[26] PyB$^+$FeCl$_4^-$, AP-TMS, CP-TMS, dimethylsulfoxide (DMSO), and glycerol were purchased from Aldrich and used as received. PyB$^+$ ions were incorporated into zeolite L crystals (3 g) by aqueous ion exchange of K$^+$ ions in zeolite L with PyB$^+$FeCl$_4^-$ (180 mL, 0.1 mM) under reflux (90 min). After rigorously washing the PyB$^+$-exchanged zeolite L with distilled deionized water, it was further washed with DMSO by soxhlet extraction for more than 24 h until no further PyB$^+$FeCl$_4^-$ was detected in the DMSO. The washing step with DMSO is highly recommended to rigorously remove the physisorbed PyB$^+$FeCl$_4^-$ salts from the external surfaces of the zeolite powders. Analysis of the amount of PyB$^+$ ions according to the method of Minkowski and Calzaferri[36] revealed that the incorporated amount corresponded to 1.7 ions per channel. Although the incorporated amount was rather low, the incorporated PyB$^+$ ions were aligned with the channel direction as reported by Calzaferri et al.[21] (see the Supporting Information for more evidence). The AP-tethered PyB$^+$-containing zeolite L crystals and CP-tethered glass (CP-g) plates were prepared according to the standard method developed in our group.[14] v-(PyB$^+$)L-g and h-(PyB$^+$)L-g were prepared by the SS method according to the procedure describe in the Supporting Information.[19]

Measurements of anisotropic photoluminescence: The setup used was basically the same as that described in the literature.[29] The layout and the detailed description is given in the Supporting Information. Three v-(PyB$^+$)L-g or h-(PyB$^+$)L-g plates were placed horizontally on a stack of five bare glass plates placed horizontally in a glass container ($20\times20\times10$ mm^3) charged with glycerol as an index-matching fluid. A vertically or horizontally polarized beam ($\lambda = 514.5$ nm) generated from an Ar$^+$ ion laser (Coherent) was introduced into the stack of v-(PyB$^+$)L-g or h-(PyB$^+$)L-g, and the produced fluorescent light was introduced into a spectrometer (Horiba Jobin Yvon, TRIAX 550) equipped with a charge-coupled device (CCD) array (1024×512) detector after passing it through an achromatic $\lambda/2$ plate to rotate the polarization to 0° and a linear polarizer fixed at 0° (horizontal). Care was taken to ascertain that the detection system did not introduce any systematic anisotropy. This was checked by analysis of PyB$^+$ dissolved in glycerol with circularly polarized laser light and obtaining the ratio of vertically polarized to horizontally polarized luminescence intensity of 1.05:1.

Received: January 8, 2006
Revised: May 17, 2006

Keywords: fluorophores · luminescence · monolayers · zeolites

---

[1] a) N. B. Bowden, M. Weck, I. S. Choi, G. M. Whitesides, *Acc. Chem. Res.* **2001**, *34*, 231; b) G. A. Ozin, *Chem. Commun.* **2000**, 419.
[2] A. Blanco, E. Chomski, S. Grabtchak, M. Ibisate, S. John, S. W. Leonard, C. Lopez, F. Meseguer, H. Miguez, J. P. Mondia, G. A. Ozin, O. Toader, H. M. van Driel, *Nature* **2000**, *405*, 437.
[3] B. T. Holland, C. F. Blanford, A. Stein, *Science* **1998**, *281*, 538.
[4] J. S. Lee, Y.-J. Lee, E. L. Tae, Y. S. Park, K. B. Yoon, *Science* **2003**, *301*, 818.

[5] Z. Li, C. Lai, T. E. Mallouk, *Inorg. Chem.* **1989**, *28*, 178.
[6] Y. Yan, T. Bein, *J. Phys. Chem.* **1992**, *96*, 9387.
[7] a) J.-W. Li, K. Pfanner, G. Calzaferri, *J. Phys. Chem.* **1995**, *99*, 12368; b) J.-W. Li, G. Calzaferri, *J. Chem. Soc. Chem. Commun.* **1993**, 1430.
[8] L. C. Boudreau, J. A. Kuck, M. Tsapatsis, *J. Membr. Sci.* **1999**, *152*, 41.
[9] P. Lainé, R. Seifert, R. Giovanoli, G. Calzaferri, *New J. Chem.* **1997**, *21*, 453.
[10] T. Ban, T. Ohwaki, Y. Ohya, Y. Takahashi, *Angew. Chem.* **1999**, *111*, 3590; *Angew. Chem. Int. Ed.* **1999**, *38*, 3324.
[11] a) S. Feng, T. Bein, *Nature* **1994**, *368*, 834; b) S. Feng, T. Bein, *Science* **1994**, *265*, 1839; c) T. Bein, *Chem. Mater.* **1996**, *8*, 1636.
[12] A. Kulak, Y.-J. Lee, Y. S. Park, K. B. Yoon, *Angew. Chem.* **2000**, *112*, 980; *Angew. Chem. Int. Ed.* **2000**, *39*, 950.
[13] S. Y. Choi, Y.-J. Lee, Y. S. Park, K. Ha, K. B. Yoon, *J. Am. Chem. Soc.* **2000**, *122*, 5201.
[14] K. Ha, Y.-J. Lee, H. J. Lee, K. B. Yoon, *Adv. Mater.* **2000**, *12*, 1114.
[15] K. B. Yoon, *Bull. Korean Chem. Soc.* **2006**, *27*, 17.
[16] G. S. Lee, Y.-J. Lee, K. B. Yoon, *J. Am. Chem. Soc.* **2001**, *123*, 9769.
[17] J. S. Park, G. S. Lee, Y.-J. Lee, Y. S. Park, K. B. Yoon, *J. Am. Chem. Soc.* **2002**, *124*, 13366.
[18] J. S. Park, Y.-J. Lee, K. B. Yoon, *J. Am. Chem. Soc.* **2004**, *126*, 1934.
[19] J. S. Lee, K. Ha, Y.-J. Lee, K. B. Yoon, *Adv. Mater.* **2005**, *17*, 837.
[20] G. Calzaferri, O. Bossart, D. Brühwiler, S. Huber, C. Leiggener, M. K. Van Veen, A. Z. Ruiz, *C. R. Chim.* **2006**, *9*, 214.
[21] G. Calzaferri, S. Huber, H. Maas, C. Minkowski, *Angew. Chem.* **2003**, *115*, 3860; *Angew. Chem. Int. Ed.* **2003**, *42*, 3732.
[22] Z. Lai, G. Bonilla, I. Diaz, J. G. Nery, K. Sujaoti, M. A. Amat, E. Kokkoli, O. Terasaki, R. W. Thompson, M. Tsapatsis, D. G. Vlachos, *Science* **2003**, *300*, 456.
[23] G. T. P. Mabande, S. Ghosh, Z. Lai, W. Schwieger, M. Tsapatsis, *Ind. Eng. Chem. Res.* **2005**, *44*, 9086.
[24] H. S. Kim, S. M. Lee, K. Ha, C. Jung, Y.-J. Lee, Y. S. Chun, D. Kim, B. K. Rhee, K. B. Yoon, *J. Am. Chem. Soc.* **2004**, *126*, 673.
[25] T. Bein, *Mater. Res. Soc. Bull.* **2005**, *30*, 713.
[26] Y.-J. Lee, J. S. Lee, K. B. Yoon, *Microporous Mesoporous Mater.* **2005**, *80*, 237.
[27] F. Marquez, C. M. Zicovich-Wilson, A. Corma, E. Palomares, H. Garcia, *J. Phys. Chem. B* **2001**, *105*, 9973.
[28] T.-Q. Nguyen, J. Wu, V. Doan, B. J. Schwartz, S. H. Tolbert, *Science* **2000**, *288*, 652.
[29] J. Wu, A. F. Gross, S. H. Tolbert, *J. Phys. Chem. B* **1999**, *103*, 2374.
[30] J. Caro, G. Finger, J. Kornatowski, J. Richter-Mendau, L. Werner, B. Zibrowius, *Adv. Mater.* **1992**, *4*, 273.
[31] C.-N. Wu, K.-J. Chao, T.-G. Tsai, Y.-H. Chiou, H.-C. Shih, *Adv. Mater.* **1996**, *8*, 1008.
[32] M. Grell, D. D. C. Bradley, *Adv. Mater.* **1999**, *11*, 895.
[33] a) H. Mass, G. Calzaferri, *Angew. Chem.* **2002**, *114*, 2389; *Angew. Chem. Int. Ed.* **2002**, *41*, 2284; b) S. Huber, G. Calzaferri, *ChemPhysChem* **2004**, *5*, 239.
[34] B. J. Schwartz, *Annu. Rev. Phys. Chem.* **2003**, *54*, 141.
[35] M. C. Lovallo, M. Tsapatsis, *Chem. Mater.* **1996**, *8*, 1579.
[36] C. Minkowski, G. Calzaferri, *Angew. Chem.* **2005**, *117*, 5459; *Angew. Chem. Int. Ed.* **2005**, *44*, 5325.